Impact fatigue in adhesive joints

V V Silberschmidt*, **J P Casas-Rodriguez,** and **I A Ashcroft**
Wolfson School of Mechanical and Manufacturing Engineering, Loughborough University, Leicestershire, UK

The manuscript was received on 25 October 2007 and was accepted after revision for publication on 15 April 2008.

DOI: 10.1243/09544062JMES924

Abstract: One of the forms of a vibro-impact effect in engineering components is impact fatigue (IF) caused by a cyclic repetition of low energy, low-velocity impacts, for instance, in aerospace structures. It can have a highly detrimental impact on performance and reliability of such components, exacerbated by the fact that in many cases it is disguised in loading histories by non-impact loading cycles with higher amplitudes. Since the latter are traditionally considered as most dangerous in standard fatigue, IF has not yet received deserved attention; it is less studied and practically unknown to specialists in structural integrity. Though there is a broad understanding of the danger of high-energy single impacts, repetitive impacting of components has been predominantly studied for very short series. This paper aims at the analysis of IF of adhesively bonded joints, which are becoming more broadly used in aerospace applications. The study is implemented for two types of typical adherends – an aluminium alloy and a carbon-fibre reinforced composite – and an industry-relevant epoxy adhesive. Various stages of fatigue crack development in adhesively bonded joints are studied for the conditions of standard and IF. The results obtained – in terms of crack growth rates, fatigue lives, and microstructures of fracture surfaces – are compared for the two regimes in order to find similarities and specific features.

Keywords: impact fatigue, adhesive, crack growth, adhesively bonded joints

1 INTRODUCTION

Prediction of performance of various structures and components under real-life loads is usually based on the models of material behaviours. These models are validated by experimental studies performed on specimens of respective materials using various types of mechanical loads (an isothermal case is considered in this paper). Such loads are a generalization of loads in service and normally limited to (quasi) static, cyclic, dynamic, creep, and relaxation. A need for these various types is linked to different responses of the same materials to various loading conditions, and there is a general understanding that results obtained in experiments of one type can hardly be sufficient to predict outcomes for other experiments. One of the obvious examples is a lesson, painfully learned by the engineering community in the nineteenth century, that (quasi-static) strength cannot be used to predict reliability of components exposed to cyclic loading (fatigue). Another example is a dynamic overshoot factor, roughly doubling the maximum magnitude of the load due to the weight if it is suddenly applied to a component.

Still, one type of the load has not yet obtained the attention, which it undoubtedly deserves. This is a repetition of low-energy impacts, with each impact being insufficient to cause the total failure of a structure or component. This type of loading is known as impact fatigue (IF) and is in the centre of this study.

It is a well-established fact [**1**] that research into IF started effectively at the same time as the one into standard, non-IF, i.e. in the middle of the nineteenth century [**2**]. More than a century ago a 'shock-fatigue' test, defined as one 'involving a large number of relatively small blows', was used to study a response of steels to this type of loading in comparison with a static test and a 'single-blow' test [**3**]. Those tests were performed with specially designed testing machines for impacts in bending, tension, and compression. The tests in bending were implemented for loading histories of up to 10^6 cycles while those for tensile impacts – 'owing to the relatively slow speed of the direct-impact

*Corresponding author: Wolfson School of Mechanical and Manufacturing Engineering, Loughborough University, Ashby Road, Leicestershire LE11 3TU, UK. email: V.Silberschmidt@lboro.ac.uk

tester' – were limited to 50 000 impacts [**3**]. A difference between effects due to IF and both single-impact loading and standard fatigue (SF) was apparent at that time as well as the absence of a durability limit (named 'limiting resistance').

Still, more than a 100 years after those conclusions, the area of IF is considerably less studied than that of the standard, non-impact one, not to mention any introduction of its notion into design regulations. There are several reasons for such a situation. One of them is ambiguity in the choice of the loading parameter. For an SF, an obvious parameter is the stress amplitude that comes back to the notion of Wöhler's S–N (i.e. stress versus number of cycles) diagrams in stress-controlled fatigue [**4**]. In IF, a maximum stress magnitude can be hardly used as a sole parameter since – depending on the loading conditions, especially impact velocity – the same level of this parameter can correspond to different levels of the applied energy. As a result, different authors have been using various loading parameters in their studies.

Another reason is the specificity of IF realization in different types of materials. Already in 1908, Stanton and Bairstow [**3**] noticed 'remarkable endurance for lighter blows' in brittle specimens. Some authors even mention a higher resistance of specimens exposed to impact-fatigue conditions as compared with SF. This can be explained by linkage between the levels of impact energy, contact duration, and damping properties resulting in a specific type of spatial localization of the stresses and their decay with propagation from the contact area. This linkage can differ with kinematics of impact-induced deformation and the specimen's geometry and type of fixture. One extreme example is shot peening, which is a repetitive impacting with tiny particles, resulting in improved fatigue performance due to strengthening of a near-surface layer [**4**]. Another example is repetitive impacting of laminated composites in drop-weight test systems [**5**, **6**], where the most affected zone is situated below the contact area, resulting in delamination initiation in this part of laminate and its subsequent spreading to other parts of tested specimens.

Hence, there are many interacting factors affecting the behaviour of components and structures under repetitive low-energy impacting. This study, aimed at a detailed analysis of IF, tries to diminish the extent of its complexity by eliminating some of these interactions. For instance, uniaxial impact loading of specimens in the study, on the one hand, avoids macroscopically non-uniform stress distributions that are characteristic for bending loading of Izod tests or lateral loading of laminates. On the other hand, the results obtained for IF can be directly compared with those for standard tensile fatigue procedures. Adhesively bonded joints were also chosen in an attempt to reduce the damage process only to a relatively weaker – as compared with adherends – layer of adhesive in order to preclude multi-mechanism damage evolution. Obviously, another – and a very strong – reason for this choice was an expanding use of adhesive joints in the aerospace industry.

Impact events that arise in aerospace structures and components due to gusts, storms, and landing can be masked in loading history diagrams, presenting thousands of loading cycles with various amplitudes. The existing methods to treat such diagrams, e.g. so-called 'rainflow technique' [**7**], are considered with a proper way of counting events, making no distinction between impacts and relatively slow cycles that can be treated as non-IF events. This can be very dangerous, since impacts with lower amplitude can be more damaging than non-impact cycles with higher amplitudes.

2 ADHESIVE JOINTS: RESPONSES TO FATIGUE AND IMPACT

New designs of aeroplanes have an increasing use of carbon-fibre reinforced (CFRP) composites alongside the continuing application of aluminium alloys. With a permanent drive to improve a strength-to-weight ratio, adhesive jointing of structural materials becomes an obvious option for parts where it can eventually replace traditional fastener joints – nuts, screws, rivets, etc. The latter not only provide a discrete bonding – contrasting to a continuous one in the case of adhesive joints – and are considerably heavier but also cause stress concentration due to perforation of joining components.

Still, application of adhesives is linked with some challenges with regard to prediction of their performance. This is a result of specific features of their microstructure as well as mechanical and damage behaviour. Structural adhesives are typically multi-component materials and hence can be considered as nanocomposites [**8**] with epoxy resins commonly used as a matrix and rubber particles and/or inorganic fillers [**9**] as toughening elements. Extensive research has been undertaken to study the effect of these inclusions on the behaviour of adhesives. Three main mechanisms responsible for this effect were established [**10**]. The first mechanism is the cavitation of rubber particles, manifested by voids (holes) in the fracture surface of the adhesive. The second mechanism is the formation of shear bands that can occur in areas with a high density of particles, contributing to the onset of plasticity. The third mechanism is bridging when rubber particles bridge a gap between crack/delamination faces thus impeding crack propagation. Obviously, the effects due to these mechanisms depend on the volume fraction and size of rubber particles [**8**].

Specificity of loading of aerospace structures, exposed to complex load histories, which are traditionally presented as combinations of blocks of cycles with different amplitudes and respective stress ratios, made fatigue in adhesive materials the most studied loading type. The main emphasis of studies by various researchers was, in general, on constant-amplitude blocks [**11**] and variable-amplitude blocks [**12**]. In those tests, the main parameters were the maximum force or stress and the load ratio; in most cases, a sinusoidal shape of load cycles has been used. In this paper, these type of experiments will be referred to as SF. Two main approaches have been used to analyse SF in adhesive joints: stress-life analysis and fatigue crack growth (FCG) studies [**13**]. The stress-life approach employs S–N diagrams to present the fatigue life's dependence on stress. Its main limitation is the lack of an explicit account of damage evolution during fatigue. The FCG approach is used to characterize an incremental crack growth per cycle (da/dn) linked to fracture mechanics parameters. Traditionally, a compliance method is used for double-cantilever joints to determine the strain energy release rate G_I in mode I; this parameter is calculated for the maximum load magnitude from the sinusoidal load curve.

Research into impact loading of adhesive joints is mostly limited to single-impact loading. Three main types of tests are used to analyse the effect of impacts: (a) experiments with pendulum impact testers with impact rates below 5 m/s; (b) drop-weight tests, with rates up to 10 m/s; and (c) a split Hopkinson pressure bar (SHPB) testing technique for rates up to 100 m/s; [**14**]. Two standard tests can be used to evaluate the impact strength in adhesives: ASTM D950-03 standard test method for impact strength of adhesive bonds and ISO 11343:2003 adhesives – determination of dynamic resistance to cleavage of high-strength adhesive bonds under impact conditions – wedge impact method. The first of these standard methods employs two bonded together blocks; the bottom block is rigidly secured in the test rig and a pendulum hammer strikes the top block, generating a shear load in the adhesive layer. The second method is an impact wedge-peel test, in which a wedge loaded by a servo-hydraulic machine cleaves the joint, producing a peeling stress in the adhesive.

So far, results of studies of adhesives under impact loading have been controversial. Some researchers report similar results for impact and quasi-static conditions, e.g. for a single-lap joint (SLJ) tested in a pendulum impact machine in reference [**15**]. In reference [**16**] higher strength was measured in impact loading; it was supposed that the result was due to the strain-rate sensitivity of the adherends that caused higher dynamic strength. An analysis of the shear response of a joint with thick adherends, subjected to various stress waves generated by impacts, showed that the type of fracture was associated with the level of the incident stress [**17**]. Another study [**18**] demonstrated a considerable extent of variability in stress states in the block-impact test caused by complex dynamic effects due to uncertainties in conditions at the contact interface between the block and the hammer. It was suggested that the impact-wedge test should be used to measure the impact properties of an adhesive. However, the results obtained in the impact-wedge test were found to depend strongly on the environmental conditions [**19**]. Investigations in the area of single impacts in adhesive joints using the SHPB test [**20**, **21**] demonstrated a considerable increase in the tensile strength magnitude with the loading rate; that also depended on the type of adherends. In that study, an optimum adhesive thickness was identified when the effect of the type of adherends vanished. Similar results were obtained in reference [**14**] showing that increases in the energy absorption at higher strain rates were observed only for some adhesives.

In contrast to the vast body of research into the single-impact loading of adhesive joints, IF has so far received very little attention. In many cases, the analysis of repetitive impacting has been limited to relatively short series of impacts. A representative study in the area of IF has been dedicated to the analysis of glass-fibre reinforced polymers (GFRP) SLJs bonded with an epoxy adhesive and tested using a drop-weight method [**22**]. It was demonstrated that IF strength of the joints depended on the stress magnitude and the loading time. In addition, a phenomenological model to predict failure in impact conditions was suggested based on the cumulative time ($N_f T$) and the maximum stress amplitude in the impact (σ_{max}) in the following form [**23**–**26**]

$$\sigma_{max}(N_f T)^m = C \tag{1}$$

where N_f is the number of cycles to failure and T is the loading time; C and m are empirical parameters of the IF model. This model will be referred in this paper as the accumulated time-stress model.

The aim of this paper is to study the effects of IF in adhesive joints by analysing the loading parameter-life relation and the FCG using different types of adherends and modified epoxy rubber structural adhesives, identifying main mechanisms responsible for the response of the adhesive to these loading conditions.

3 EXPERIMENTAL STUDIES

3.1 Materials

Two types of adherends are used in the experimental studies – an aluminium alloy for fatigue-life experiments and a CFRP composite for FCG experiments.

The aluminium alloy is 7075-T6 in clad conditions with thickness of 2.5 mm. The CFRP composite used is T800/5245C, supplied by Cytec Limited. The composite's matrix, Rigidite 5245C, is a modified bismaleimide/epoxy system reinforced with T800 carbon fibres supplied by Toray Industries Limited. The composite panels are laid-up from a unidirectional prepreg plies with thickness 0.125 mm and a volume fraction of fibres 0.6; a multi-directional lay-up scheme $[(0/-45/+45/0)_2]_S$ is also used in experiments. CFRP panels were cured for 2 h at 182 °C with an initial autoclave pressure of ≈600 kN/m^2; the cured panels were ultrasonically scanned to detect defects.

Two various adhesives are used in two types of tests. The adhesive/primer combination used in fatigue-life specimens with aluminium adherends is an FM 73M/BR 127 system from Cytec Limited. The film adhesive FM 73 is a single-part, toughened epoxy film adhesive supported by non-woven polyester fibres, which control the glue thickness and flow during the curing. The primer BR 127 is a modified epoxy-phenolic consistent of 10 per cent solids including 2 per cent strontium chromate as a corrosion inhibiting additive. The adhesive used for FCG specimens is Hysol Dexter's EA-9628, which was supplied as a 0.2 mm thick film. This adhesive is based on a diglycidyl ether of bisphenol A with a primary amine curing agent. A reactive liquid polymer, based on carboxyl terminated butadiene acrylonitrile rubber, is used as a toughening agent.

3.2 Preparation of specimens

The main objective of the experimental studies is comparability of the results obtained for two types of loading conditions – standard (i.e. non-impact) fatigue and IF. As two types of tests are performed with the use of two testing machines, each with its own clamping arrangement, design of specimens should, on the one hand, account for these differences and, on the other hand, provide similarity of the major features of specimens, namely, the joint preparation procedure and length of the adhesive layer. SLJ specimens are used in the evaluation of SF; they were prepared following EN ISO 9664:1995 adhesives – test methods for fatigue properties of structural adhesives in tensile shear.

3.2.1 Fatigue-life specimens

Specimens with aluminium-alloy adherends (shown in Fig. 1(a)) were manufactured in three stages. At first, a grit-blasting pretreatment of surfaces of aluminium-alloy plates was carried out, employing alumina particles with dimensions 200 μm under pressure 55 kPa with a working distance 15–20 cm. Such pretreatment increases the contact area between the adhesive and adherends, improving a mechanical interaction between these two components [**27**]. The next stage is a degreasing process with acetone: aluminium plates are placed into acetone and exposed to ultrasound for 5 min. This process is repeated twice before the last stage – joining. At this stage, a thin film of BR 127 primer is applied to the bond area and dried for 30 min at room temperature and then cured at 120 °C for 30 min. A sheet of FM 73 M is then cut into pieces 12.5 × 26 mm. One piece of adhesive is placed at the overlap between the adherends for each sample, and any excess adhesive is cut off. Bonding is achieved by fixing the adherends using clamps and curing for 60 min at 120 °C.

3.2.2 FCG specimens

The lap-strap joint (LSJ) specimens (Fig. 1(b)) are assembled using precured CFRP laminate adherends and EA-9628 adhesive. Joints are cured in an autoclave for 60 min at 120 °C. The final shape of specimens is obtained by cutting the bonded panels using a diamond saw. End tabs for the specimens are made of 7075-T6 aluminium alloy and bonded to specimens with FM-73 adhesive. Holes were drilled in the specimens used for the IF tests using three drills with increasing diameters to minimize the possibility of delamination in the composite.

3.3 Testing equipment and procedures

A servo-hydraulic fatigue testing machine with digital control and data logging was used in quasi-static and SF tests. A main loading parameter for quasi-static loading conditions is the maximum force $F_{\max}^{\text{static}}$ that was obtained by averaging maximum load values attained by two specimens tested at tension with a displacement rate of 0.05 mm/s. All the SF tests were conducted in a force-control regime, with a load ratio (minimum to maximum load) $R = 0.1$ and frequency 5 Hz. The maximum load in fatigue-life test varied; in FCG tests the load amplitude was 60 per cent of $F_{\max}^{\text{static}}$.

For IF tests, a modified CEAST RESIL impactor was used as described in detail in reference [**28**]. In these experiments a specimen is fixed at one end to an instrumented vice and a special impact block is attached to its free end. The impact by a pendulum hammer produces a tensile load in the specimen for a short interval. In the IF test the pendulum hammer is released from a preselected initial angle; this angle is kept constant during the entire series of impacts. Changing this position as well as a mass of the attached weight, it is possible to attain the magnitudes of the initial potential energy in the range of 0–4 J and the impact velocity between 0 and 3.7 m/s. Evolution of forces, displacements, and the energy during each impact can be monitored for 5 μs and acquired for up to 8000 points. Fatigue-life experiments for IF were

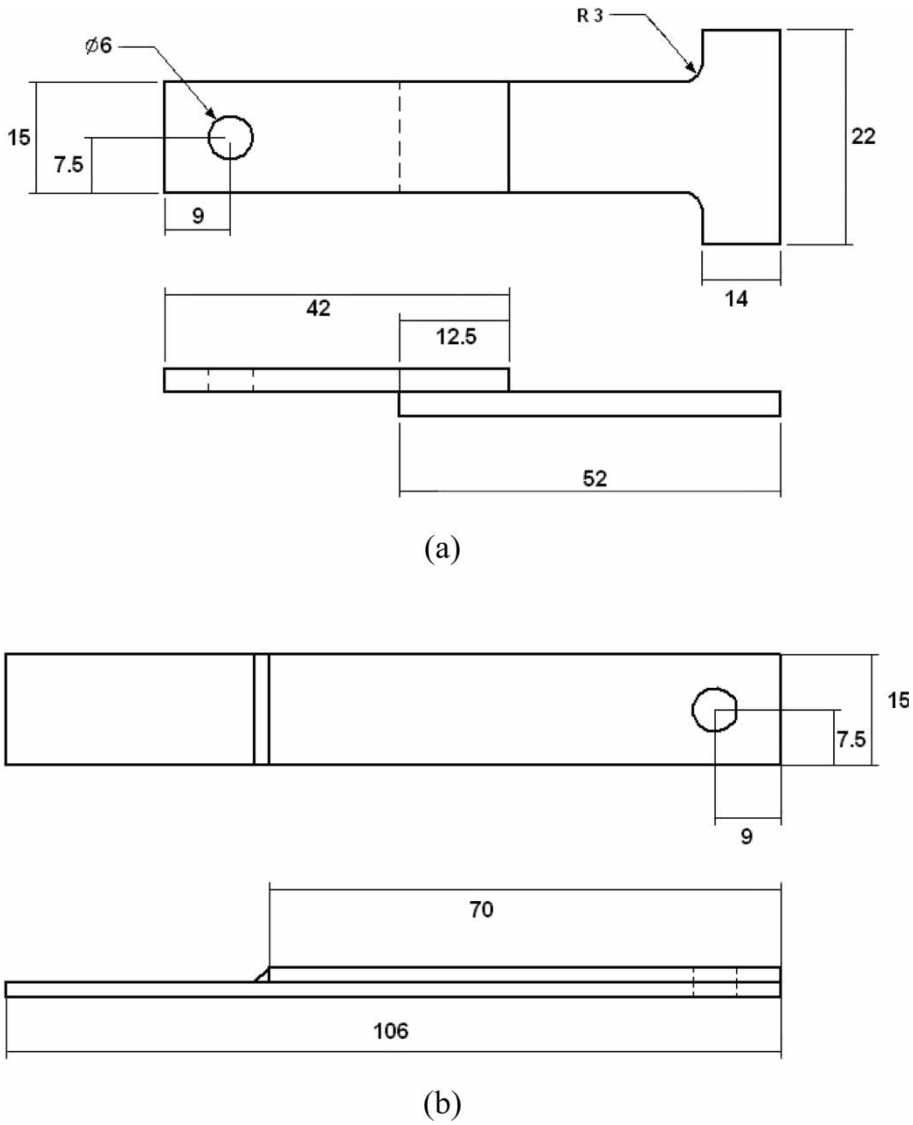

Fig. 1 Specimens for experimental studies: (a) SLJ and (b) LSJ. Dimensions in millimetre

performed using several specimens so that a complete force-life (i.e. number of impacts to failure) diagram could be obtained. The process of FCG under IF conditions was studied using a constant initial potential energy for all tested specimens.

All tests were performed in ambient laboratory conditions. After mechanical testing, fracture surfaces of failed specimens were examined with an optical microscope. High-magnification studies were also performed using a scanning electron microscope (SEM). In the latter case, fracture surfaces were gold-coated prior to SEM examination with a voltage range 15–25 kV.

The process of FCG in SF was examined by means of *in situ* crack measurements. A system of marks was produced for all specimens with a vernier calliper on the white painted surface of the specimens' edges as a reference. The crack size was then measured using portable optical microscopy for both edges in all specimens. Measurements of crack lengths in the IF tests were carried out using optical microscopy, with computer-controlled halting of the test after a prescribed number of impacts so that the specimen could be studied. Captured digital images were used to measure the crack size.

4 RESULTS

4.1 Stress-life approach

An obvious starting point of the research into the response of specimens to cyclic external loads is the analysis of the effect of the loading factor on the life of specimens. Though a stress magnitude is a more convenient loading parameter that provides a measure independent of the specimen's dimensions (i.e. of its respective cross-section), it cannot be used for the

types of specimens under study. Previous research into adhesive joints demonstrated that the shear and peel stresses in adhesives are distributed non-uniformly over the bonding area, with peak values near the fillets. In order to exclude an ambiguity in the analysis, the force magnitude is selected as a loading parameter. Thus, a force versus number of cycles diagram (Fig. 2) is used as one of the tools to compare two fatigue regimes – SF and IF; the maximum load magnitude is normalized by the quasi-static load $F_{\max}^{\text{static}}$.

The experimental results obtained for SF show an increase in the number of cycles to failure with a decreasing normalized force. A fatigue limit defined for 10^6 cycles is reached when specimens are tested at 30 per cent of their quasi-static strength. Results for IF conditions demonstrate that load amplitudes for the same fatigue life parameters are significantly lower, in most cases they are below the standard-fatigue limit. An obvious trend of an increasing fatigue life with a decreasing load parameter is also present in IF.

As was discussed above, the magnitude of the maximum force is not suitable as the only parameter, characterizing impacts, as it can be the same for impacts with various durations. Thus, a measure of energy should be additionally used to characterize the effect of IF. Figure 3 presents a relationship between the absorbed energy $\bar{E}_t$ per impact in a specimen, averaged over the entire number of N cycles of the loading history; this type of diagram will be referred to as an E–N diagram. This diagram has two portions with significantly different slopes: the extent of decrease rate necessary to increase the fatigue life is considerably lower for lives more than 10^3 impacts.

Both S–N and E–N diagrams vividly justify that a decrease of the respective maximum loading parameter for quasi-static (or single-impact) loading conditions, even by an order of magnitude, which is more than enough for SF, does not guarantee safety for a component or structure in the repetitive impacting regime.

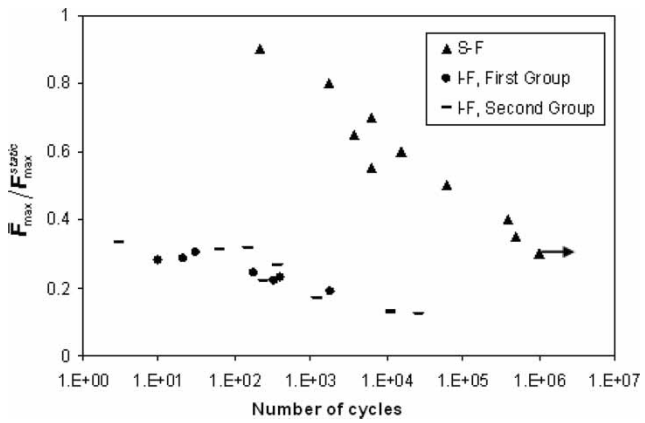

Fig. 2 F–N diagrams for aluminium joints for impact and SF

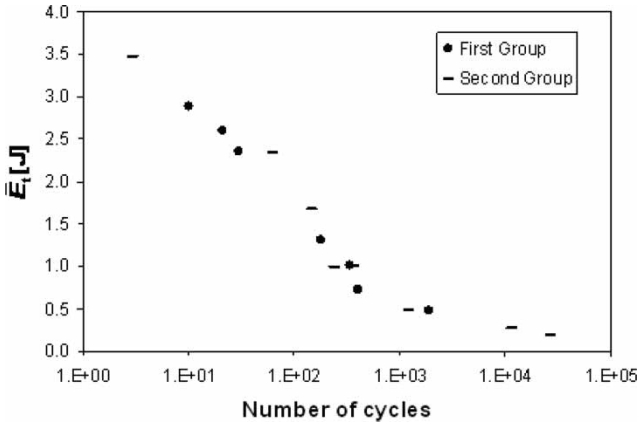

Fig. 3 E–N diagram for IF

4.2 Fatigue crack growth

The study of the FCG behaviour in adhesively bonded joints demonstrates a pronounced variability of crack growth scenarios in specimens, prepared in the same way from the same materials and loaded under similar conditions. This variability is known to the fatigue community to be responsible for a large scatter in the fatigue life.

LSJs were used in this study; failure in LSJ specimens (Fig. 1(b)) is defined as the moment when the crack reaches a length of 40 mm, measured from the fillet. The necessity to introduce such definition is due to clamping of the edge, opposite to the fillet. In SF, two main kinds of FCG behaviour are observed: slow and accelerated crack (delamination) propagation (Fig. 4). A traditional diagram relating the crack length to the respective number of cycles (Fig. 4(a)) is insufficient for an adequate analysis, as fracture evolves differently in various specimens, and stress concentrations can vary considerably for the same number of cycles due to different crack lengths in specimens. To overcome this, another diagram visualizing the crack growth rate at different stages of FCG (in terms of the crack length) is introduced (Fig. 4(b)). In this diagram, it is apparent that the initial stage of different types of FCG is similar when the crack propagates with the rate around 3×10^{-4} mm/cycle and maintains a continuing decreasing trend until it reaches a length of 20 mm. After this, an increase in the crack growth rate is observed in the accumulated FCG while the decreasing trend continues, practically with the same slope, for the slow FCG (Fig. 4(b)). As a result, the difference in the crack growth rate for these two types reaches nearly two orders of magnitude before failure.

The same graphic tools are used to analyse the crack growth process in LSJ in IF conditions (Fig. 5). Though

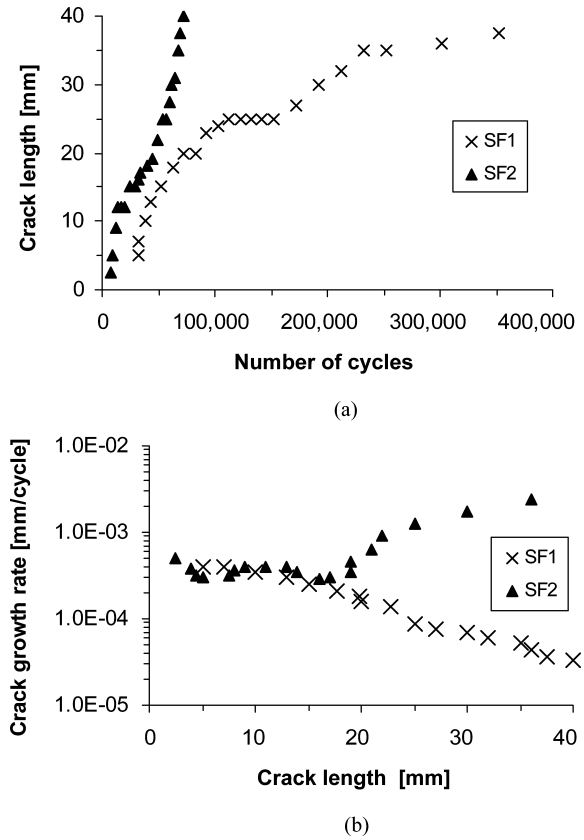

Fig. 4 Fatigue behaviour in LSJs tested in SF: (a) crack growth and (b) crack growth rate

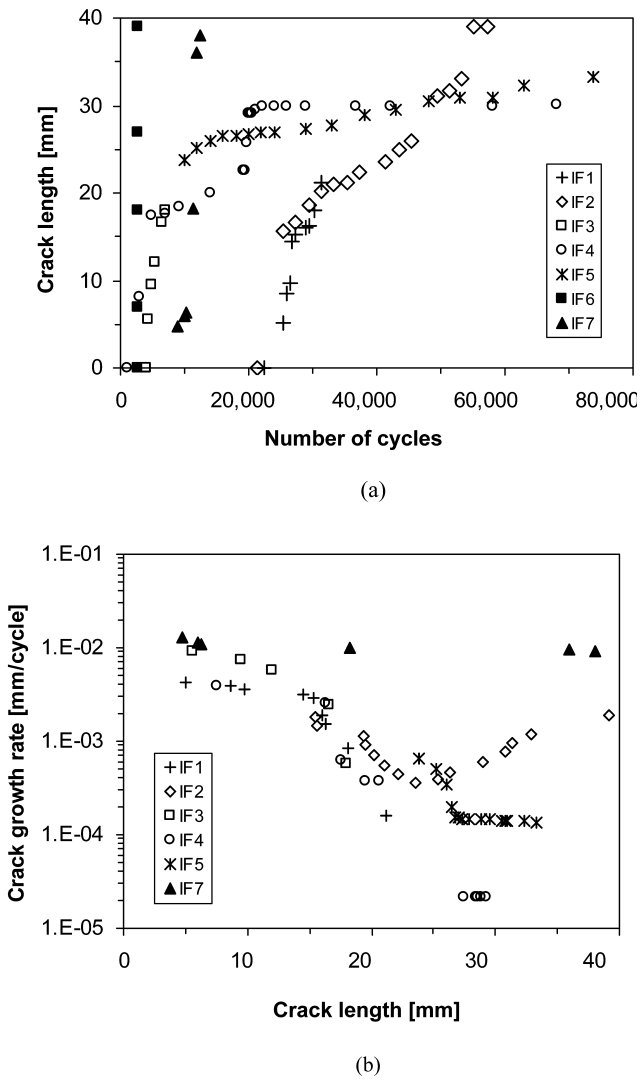

Fig. 5 Fatigue behaviour in LSJs tested in IF: (a) crack growth and (b) crack growth rate

the scatter here is considerably higher, the obtained results can also be divided into two main groups based on the FCG behaviour. In the rapid FCG found in two specimens – IF6 and IF7 – the entire specimens' lives are comparable – and even shorter – than a crack initiation stage for other specimens (Fig. 5(a)). The crack growth rate in this case is above 10^{-2} mm/cycle over the entire fatigue life (Fig. 5(b)). On the other hand, the slow FCG behaviour is found in other specimens. This behaviour has some general features – the initial stage of crack propagation in these specimens, which lasts until a crack length of 15 mm is reached, is characterized by a nearly constant crack speed at the level somewhat below 10^{-2} mm/cycle. After this stage, a decrease in the crack growth rate is noticeable. This decelerating FCG changes when the crack reaches a length of $\approx$27 mm, when a constant-rate plateau is attained (though one specimen demonstrated an accelerated crack growth instead). The crack rates magnitudes at this stage can vary considerably – from 10^{-4} to 2×10^{-5} mm/cycle.

The pronounced variability of the obtained crack growth scenarios in IF vividly manifests a multi-mechanism character of damage in adhesively bonded joints. The behaviour is by no means chaotic – the same levels of instantaneous crack growth rates are continuously reproduced during thousands of impacts and in various specimens.

An additional parameter is used to characterize the FCG in IF tests – energy E_n^* accumulated over the nth cycle

$$E_n^* = \int_{t_n^s}^{t_n^e} F_n(t) v_n(t) \mathrm{d}t \tag{2}$$

where t_n^s and t_n^e are moments of the start and end of the nth cycle, respectively; F_n is the force and v_n is the velocity. A graph of the change of E_n^* normalized by the initial potential energy of the hammer E_0 with the number of cycles (impacts) is shown in Fig. 6. It is apparent that at the first stage below 1000 cycles the introduced parameter is effectively constant. However, E_n^*/E_0 decreases rapidly between 1000th and 3000th cycles, which is consistent with the onset of macrodamage propagation in the joint. It should be

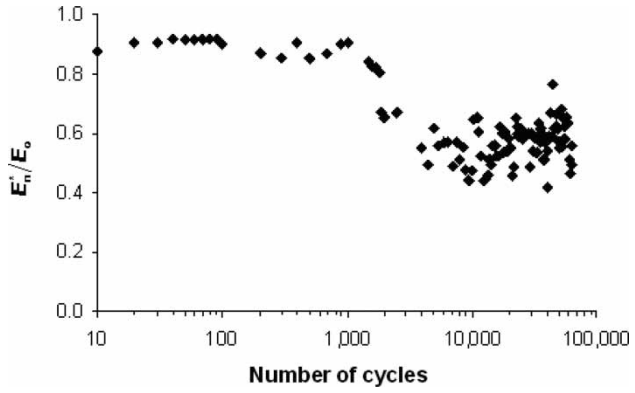

Fig. 6 Changes in the normalized accumulated energy during crack growth in IF

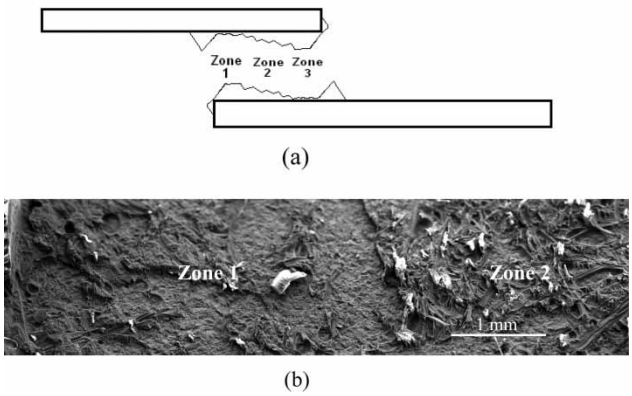

Fig. 7 Detail of the failure in mixed fracture path in SF: (a) schematic and (b) SEM

noted that the difference between E_0 and E_n^* cannot be used to calculate directly the energy used to create new fracture surfaces, as additional sources of energy dissipation are present in the system. Nevertheless, this difference can still be employed as a useful reference value of the energy associated with the crack growth process as this is considered the principal source of energy consumption.

Mechanical and energy considerations cannot provide an unambiguous explanation of the reasons for the observed variety of crack-growth behaviours in bonded joints due to the interaction of multiple factors involved in the process of damage growth. Hence, they should be accompanied by a microstructural analysis of fracture surfaces in order to obtain an additional insight into the process.

5 FRACTOGRAPHY ANALYSES

5.1 Fatigue-life tests

In SLJ specimens with aluminium-alloy adherends tested in SF and IF, SEM analysis of fractured surfaces shows two main failure scenarios: cohesive failure and mixed-mechanism fracture paths. However, quasi-similar fracture surfaces are found for principally different levels of loading conditions for these two types of fatigue. For instance, cohesive fractures in SF specimens are observed when the maximum force magnitude of the sinusoidal load graph is above 65 per cent of the quasi-static strength $F_{\max}^{\text{static}}$. This type of fracture behaviour is present in IF when the average absorbed energy per impact is higher than 0.5 J (it corresponds to the slope change in Fig. 3) that is equivalent to the maximum load force of approximately 20 per cent of $F_{\max}^{\text{static}}$.

On the other hand, the mixed-mechanism fracture path is observed in specimens tested at medium force levels in SF conditions and low-energy impacts. Three zones can be detected and differentiated by the fracture mechanisms responsible for them (Fig. 7(a)). In general, an interface failure of zone 1 is followed by predominantly cohesive failure that characterizes zone 2 (Fig. 7(b)). Finally, zone 3 is identified and related to as an interface failure but near another adherend. The presence of these macroscopic zones representing various failure mechanisms signifies variability of FCG regimes with different crack growth rates measured in mechanical tests. An even better insight into failure development can be provided by a microscale analysis.

This analysis shows that, in general, SF voids on the surface are present in most parts of the area including small cavities – the product of the rubber cavitation process (Fig. 8). However, in IF conditions the cavitated fracture surface is sometimes interrupted by areas of a brittle adhesive failure having a relatively smooth surface due to a lack of void formation process. Previous studies [**29**] found that in unstable regions (fast FCG) rubber particles can remain intact, resulting in an indistinct difference between the epoxy matrix and the rubber. It was shown in reference [**30**] that under certain load conditions the cavitation process can be suppressed; no differences in the fracture toughness between modified and unmodified epoxy were found in that case. That behaviour was explained as a consequence of the decrease of the shear banding effect due to insufficient levels of plastic deformation caused by rubber particles.

Additional analyses of fracture surfaces in specimens exposed to two different types of fatigue show differences of failure in the carrier fibres in the adhesive (Fig. 9). It was mentioned before that carrier fibres are not a structurally important element of the adhesive, however, the type of their failure provides an additional insight into the character of failure that happens in the adhesive. It is found that in SF fibres have oblique planes of fracture with high deformations of some fibres; in contrast, a transverse fracture in planes

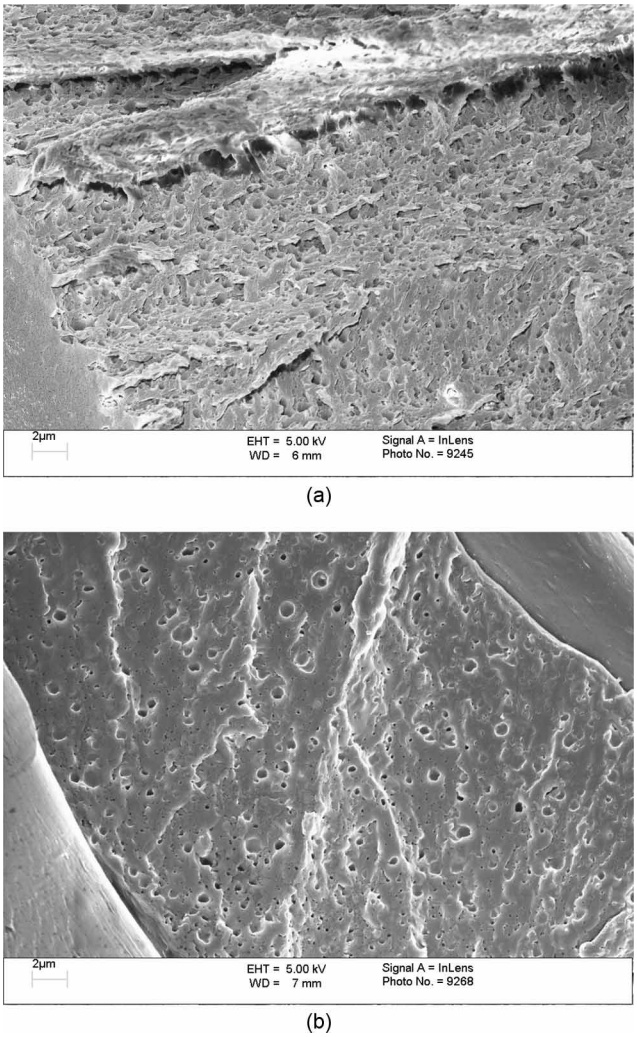

Fig. 8 Comparison of cohesive failure in SLJs: (a) SF, $F_{\max}^{\mathrm{SF}} = 5\,\mathrm{kN}$ and (b) IF $\bar{F}_{\max} = 1.8\,\mathrm{kN}$

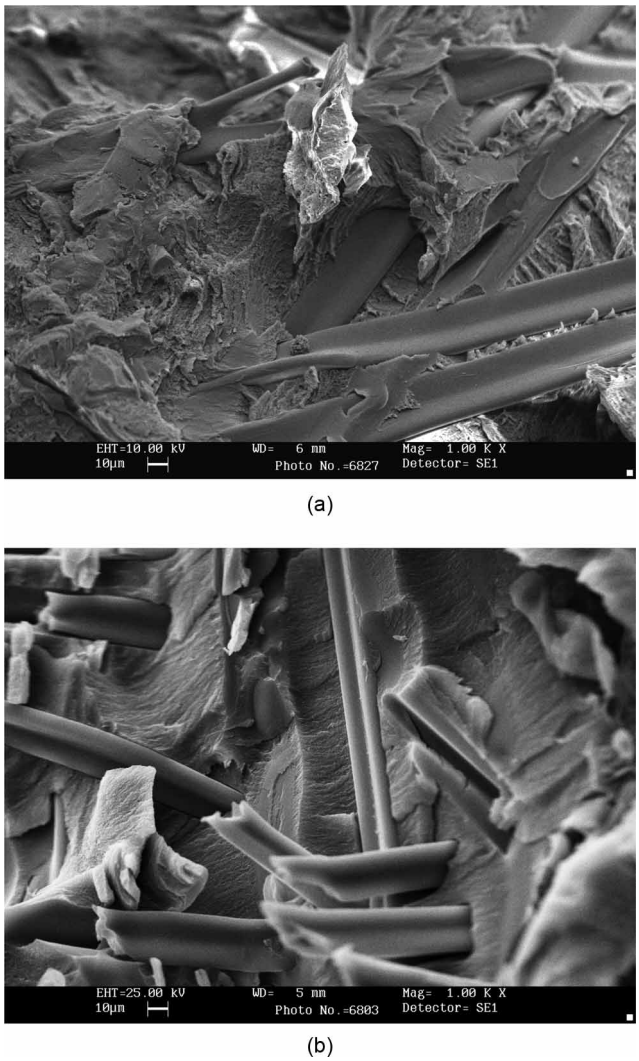

Fig. 9 Cohesive fracture paths in SLJs in SF (a) and IF (b)

nearly perpendicular to the axis of fibres is observed for specimens tested in IF. These differences can be explained by varying levels of crack propagation rates: the slow FCG is determined by plastic deformation, whereas a rapid FCG is linked with a brittle response of the adhesive.

5.2 FCG tests

Microstructural analysis of the fracture surfaces of LSJs with CFRP adherends demonstrates even more complex types of fracture than aluminium alloy-based adhesive joints. This is naturally explained by the fact that the failure in this system is not entirely limited to the adhesive layer and its interfaces, as in joins with aluminium-alloy adherends.

LSJ specimens tested under SF conditions demonstrate the presence of two main macro-mechanisms of failure. The first is cohesive failure in the adhesive layer over the entire fracture surface and related with the slow FCG (specimen SF1 in Fig. 5). The second is a mixed-mechanism fracture path, related with the fast FCG (specimen SF2 in Fig. 5). In this type of fracture, three different regions are vivid on fracture surfaces of the failed specimen (Fig. 10). The first region (region I in Fig. 10) corresponds to cohesive failure in the adhesive layer in the area close to the delamination initiation site. A second region (region II) is a transition region, in which a combination of failures both in the adhesive and in the 0° ply of CFRP, adjacent to the adhesive, is seen. In region III, the failure process is dominated by fracture in the CFRP ply adjacent to the adhesive.

Specimens, exposed to IF conditions, predominantly demonstrate the mixed-mechanism fracture paths quasi-similar to those found for SF conditions for the fast FCG. However, it should be emphasized that IF specimens are tested with peak loads of approximately 11 per cent of the quasi-static failure load of the joint as compared with 60 per cent for SF. It is seen that even at this low-load level a considerable

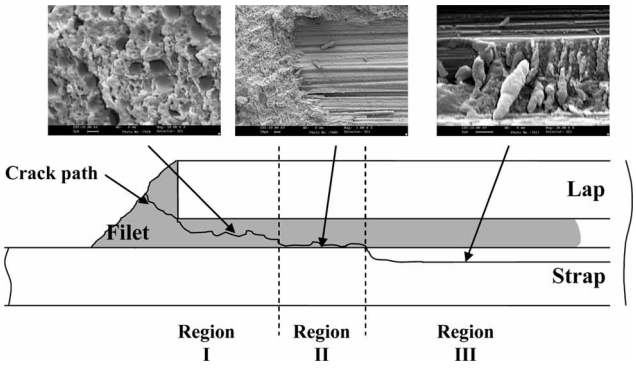

Fig. 10 Crack propagation in LSJ in SF

amount of damage occurs in the joint after relatively few cycles. The respective regions on the fracture surfaces for the mixed-mechanism fracture path in LSJ specimens with CFRP adherents are denominated A, B, and C (Fig. 11). These regions correspond to different interacting damage mechanisms and represent cohesive, combined adhesive/composite, and composite fracture regions, respectively. Though a similar transition from cohesive fracture to composite one is observed in specimens exposed to SF, realization of damage/fracture mechanisms in them is different under IF conditions. Hence, another notation – A, B, and C instead of I, II, and III – is introduced to emphasize the differences. Below, respective regions of specimens exposed to SF and IF are compared pairwise in order to elucidate the specificity of the effects due to IF.

In region A, in IF specimens the failure is ductile tearing with void formation by cavitation of rubber particles. In addition, a 'wavy' fracture surface is detected being a result of the mixed-mode fracture process. In contrast, the corresponding region I in SF specimens is characterized by a lack of cavitating rubber particles. Previous research in this area [**30**] shows that under certain load conditions the cavitation process can be suppressed, and no difference in the levels of fracture toughness can be found for modified and unmodified epoxies. Such behaviour was explained as a consequence of the decrease of the shear banding effect due to an insufficient level of plastic deformation caused by rubber particles for an instable crack growth.

Analysis of region B in the fast FCG process in IF specimens shows that this region exhibits a non-homogenous fracture behaviour (Fig. 12). This behaviour is characterized by the presence of 'islands' caused by changes in the fracture path, when the crack enters the adjacent composite with a fracture mechanism transition from cohesive failure to damage in CFRP, and later returns to the adhesive (i.e. reverting to the cohesive failure mode). One of the explanations for this behaviour is nucleation of microcracks in front of the main crack front (also known as secondary delamination zones in adhesive layers [**31**]), generating a local pattern of failure that could later merge with the main crack after it deviates into the composite. The presence of such distinct islands makes region B different from its counterpart – region II – in SF specimens (see an inset in Fig. 10).

Finally, a comparison between regions III in SF and C in IF is undertaken, demonstrating specific features of fracture development. Failure in SF is characterized by the presence of rollers and deformed shear cusps of the matrix (Fig. 10). Shear cusps are related to mode-II load that can be transformed into matrix rollers during the continuous fretting of surfaces in fatigue. Some fibre breakages are also present in region III. However, the main crack front does not break through the fibres and, hence, remains in the plane parallel to the interface between the adhesive and adherend. On the other hand, micrographs from region C of specimens tested under IF conditions show that the fracture of fibres is more common in this case (Fig. 13(b)). In contrast to SF, the shear cusps are more randomly distributed in the matrix and have, in general, signs of a more brittle behaviour, as apparent in Fig. 13.

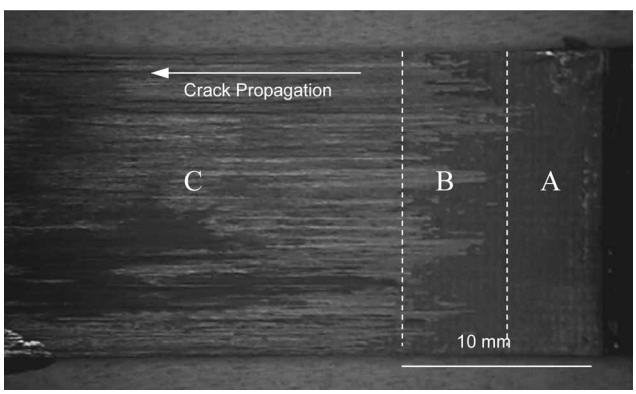

Fig. 11 Fracture surface of a specimen tested in IF

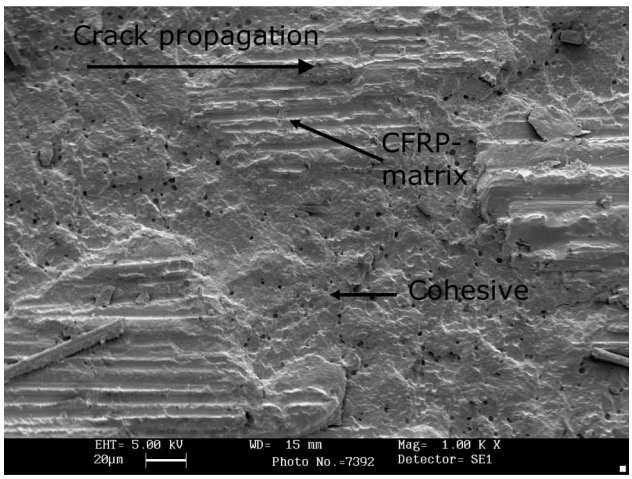

Fig. 12 Details of failure in region B for IF specimens with fast FCG behaviour

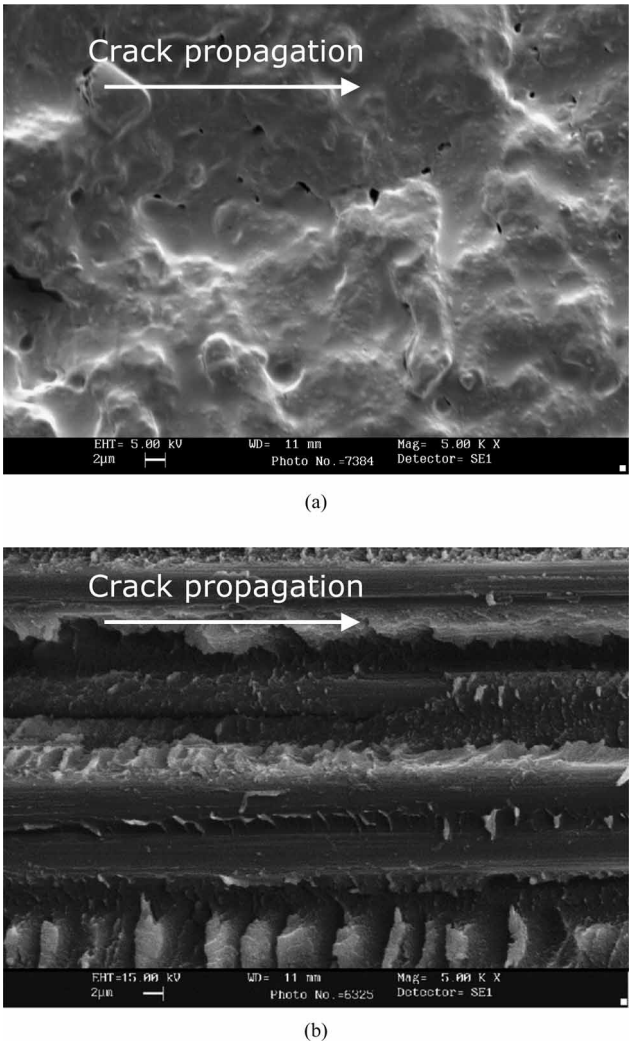

Fig. 13 SEM of fracture surfaces in samples tested in IF: (a) region A and (b) region C

6 DISCUSSION

One of the main features of crack propagation under IF conditions is a significant level of scatter even for similar specimens exposed to the same loading conditions. It is well known that the FCG is highly sensitive to geometric parameters, material's properties, local stress, and strain fields, among others factors. It is stated in reference [**32**] that the time and size scales also affect this process and, hence, should be included into the analysis of cracks that are initiated at the microscopic scale but later extended to the macroscopic one. The SEM studies of fracture surfaces of specimens failed in IF conditions demonstrate drastic differences in the type of adhesives fracture surfaces, mixed composite-matrix at the microscale, that could be responsible for higher FCG rates at the macroscale than that in specimens failed in SF conditions. It should be emphasized that the accelerated crack growth in IF is observed for levels of loads (in terms of the maximum load magnitude of the cycle) that are significantly lower than the respective parameters for SF.

SEM shows that the structure of adhesives, which are nanocomposite materials, also affects the character of crack propagation.

A starting point to consider the specificity of the effect of IF could be its comparison with high-frequency SF – the loading time for a single cycle of fatigue with a positive stress ratio and frequencies around 500 Hz (some 2 ms) would correspond to the respective parameter at IF loading (the SF experiments were performed at 5 Hz). It was shown in studies of SF at variable frequencies (between 0.25 and 25 Hz) [**33**] that a decrease in the frequency reduces the threshold value of $G_{\max}$ and accelerates the crack growth in toughened adhesive joints. This behaviour is attributed to visco-elasticity of polymer materials that are susceptible to creep. This is additionally justified by an increase in the load application time in experiments performed at positive load ratios and low frequency, making the effect of creep behaviour more prominent. The results on IF demonstrate that the FCG in adhesive joints is higher than for tests carried out in SF conditions, notwithstanding a considerably lower magnitude of the force reached in each impact. This behaviour contradicts the conclusions of reference [**33**]; the effect of accumulated creep in IF would have a smaller effect than in SF.

Another mechanism that can be responsible for specific features of cracking in adhesives was suggested in reference [**34**]. It is hysteretic heating during the loading–unloading cycle in fatigue testing of toughened adhesive joints that can affect the adhesive properties around the crack tip. It is well known that increases in temperature, especially near the glass transition range, can significantly change the mechanical behaviour of epoxy materials. Still, temperature measurements performed on the surface of specimens using thermocouples do not show considerable differences during their fatigue life. This demonstrates that hysteretic heating cannot be one of the main mechanisms affecting the character of failure in tested adhesively bonded joints.

As mentioned above, modified epoxy adhesives are visco-elastic materials, and in bulk specimens, they demonstrate a weak load-rate dependence of the Young's modulus at room temperature. This causes increase both in the yield point and maximum strength found when the loading rate grows, resulting in a diminishment of a plastic zone. It is explained in reference [**25**] that this decrease of the plastic zone is because the shear-band formation mechanism is affected by the loading rate. This means that in the case of toughening by rubber particles, an incubation

time is needed for an onset of the plastic behaviour. Hence, at very high loading rates, the adhesive will behave in a way similar to a pure epoxy adhesive. Effects of the plastic zone size on the FCG in adhesives were analysed in reference [**35**], and it was concluded that the decrease in that parameter causes a decline in material's resistance to the FCG. This effect explains the observed accelerated crack growth in adhesives in IF – as compared with SF – though their dynamic strength can be higher (in single-impact tests) than quasi-static strength.

Still, the significant decline in the dangerous loading factors (levels of applied stresses or energy), accelerating the failure process in IF as compared with standard-fatigue conditions, can hardly be explained in terms of a single-factor effect. An interaction of several mechanisms, acting at various time and space scales, is responsible for this. A high-strain-rate loading regime, characteristic to impacting, results in a more brittle response of the adhesive (and adherends), increasing its propensity to generation of microdefects – microcracks and secondary delamination zones. These defects, though being predominantly limited to the process zone within the vicinity of the propagating crack front, are randomly distributed and can be initiated both in the volume of the adhesive layer, at – or near to – adhesive–adherend interfaces and even inside the adherends – in the case of CFRP ones. Each impact within a series causes propagation of a rapidly decaying stress wave that interacts with (i.e. reflects from and/or propagates through) these defects as well as with the existing macroscopic crack. These complex interactions affect dynamics of the FCG and can be responsible for 'switching' between various damage mechanisms, depending on their respective state of development.

A relatively short range of these mechanisms, which are mostly limited to the process zone, result in a quasi-stable propagation of delamination at some stages (where there is no changes between mechanisms) with a practically constant crack growth rate for thousands of impacts.

Another important factor that causes a more rapid failure process under conditions of IF than in SF and quasi-static loading is a more effective use of energy in dynamic fracture processes. It is well known [**36**] that while in quasi-static loading a large part of energy is used to stretch the entire specimen, in dynamic loading it is effectively concentrated near the crack tip, making it easier for a crack to propagate.

7 CONCLUSIONS

A detailed comparative analysis of SF and IF in adhesively bonded joints has vividly demonstrated that the latter loading regime is considerably more dangerous. One of the most prominent features of IF is its potential to initiate a crack – and to cause its rapid propagation – at the levels of loading factors that are significantly lower than quasi-static and dynamic strengths and even the durability limit of joints. It is especially important as this range of loads is considered as safe for components exposed to cycles with varying load amplitude. These features can be visualized by means of load–number of cycles (S–N) or energy–number of cycles (E–N) diagrams that can play an important part in design of components exposed to repetitive impacting.

A large scatter in the experimental data on the crack growth in specimens tested in IF is naturally explained by multi-mechanism damage/failure scenarios, typical for adhesive joints (especially, with composite adherends). It may be noted here that high variability can also be observed in non-IF of such joints. The ways to deal with this seemingly chaotic data are suggested. First, the respective experimental data can be divided into two main groups for specimens with slow or rapid FCG resulting in a considerably lower scatter within the groups. Second, combining this analysis with, on the one hand, the crack growth rate versus crack length data and, on the other hand, detailed microstructural studies, provides an important insight into the reasons for this scatter. Microstructural analysis vividly demonstrates a diversity of microscopic features, involved in damage and failure processes. Obvious multiple 'islands' present on the fracture surfaces signify results of 'switching' damage mechanisms, when the crack propagation deviates from the adhesive layer, 'diving' into adjacent composite and returning back.

Such developments are possible due to the spatially random distributions of microdefects that make some paths more preferable for crack growth, or due to development of a larger defect in front of the crack and its merge with the propagating discontinuity. In the latter case, when secondary defects are initiated inside composite adherends, this can even cause breakage of fibres separating two defects that – under different conditions (quasi-static or non-impact cycling) – could have probably remained intact.

Attributing specific parts of the fracture surfaces to the respective stages and/or mechanisms of damage and crack growth as well as to specific portions of crack growth or crack rate diagrams provides researchers with a possibility to better understand single mechanisms as well as transitions between them. This knowledge could be invaluable for the design of safe components that are exposed to repetitive impacting during their life in service. This can be achieved not only by means of respective adjustments to safety factors but also by affecting the inherent properties of the adhesive bonds in the course of their manufacturing, e.g. changing the interface

by premanufacturing surface treatment, improving toughening mechanisms, and choice of more suitable combinations of mechanical properties of adhesives and adherends.

ACKNOWLEDGEMENT

The authors are very grateful for a partial financial support by the Royal Society within the framework of its International Joint Projects scheme.

REFERENCES

1 **Johnson, A. A.** Impact-fatigue – an emerging field of study. *Eng. Integrity*, 2004, **15**, 14–20.
2 Report of the commission appointed to enquire into the application of iron to railway structures, vol. 2, London, 1849.
3 **Stanton, T. E.** and **Bairstow, L.** The resistance of materials to impact. *Proc. Instn Mech. Engrs.*, 1908, **75**, 889–919.
4 **Hertzberg, R. W.** *Deformation and fracture mechanics of engineering materials*, 4th edition, 1996 (John Wiley & Sons, New York).
5 **Jang, B. P., Kowbel, W.,** and **Jang, B.** Impact behaviour and impact-fatigue testing of polymer composites. *Compos. Sci. Technol.*, 1992, **44**, 107–118.
6 **Schrauwen, B.** and **Peijs, T.** Influence of matrix ductility and fibre architecture on the repeated impact response of glass-fibre-reinforced laminated composites. *Appl. Compos. Mater.*, 2002, **9**, 331–352.
7 **Khosrovaneh, A. K.** and **Dowling, N. E.** Fatigue loading history reconstruction based on the rainflow technique. *Int. J. Fatigue*, 1990, **12**, 99–106.
8 **Isik, I., Yilmazer, U.,** and **Bayram, G.** Impact modified epoxy/montmorillonite nanocomposites: synthesis and characterization. *Polymer*, 2003, **44**, 6371–6377.
9 **Azimi, H. R., Pearson, R. A.,** and **Hertzberg R. W.** Fatigue of hybrid epoxy composited: epoxies containing rubber and hallow glass spheres. *Polym. Eng. Sci.*, 1996, **36**, 2352–2365.
10 **Kinloch, A. J.** Adhesives in engineering. *Proc. Instn Mech. Engrs, Part G: J. Aerospace Engineering*, 1997, **211**, 307–335.
11 **British Standards Institute.** Adhesives-test methods for fatigue properties of structural adhesives in tensile shear. 1995, BS 9664 1995.
12 **Erpolat, S., Ashcroft, I. A., Crocombe, A. D.,** and **Abdel-Wahab, M. M.** A study of adhesively bonded joints subjected to constants and variable amplitude fatigue. *Int. J. Fatigue*, 2004, **26**, 1189–1196.
13 **Ashcroft, I. A.** Fatigue. In *Adhesive bonding science, technology and applications* (Ed. R. D. Adams), 2005, pp. 209–239 (Woodhead Publishing Limited, Cambridge, England).
14 **Bezemer, A. A., Guyt, C. B.,** and **Vlot, A.** New impact specimen for adhesive: optimization of high-speed-loaded adhesive joints. *Int. J. Adhesion Adhes.*, 1998, **18**, 255–260.
15 **Harris, J. A.** and **Adams, R. D.** An assessment of the impact performance of bonded joints for use in high energy absorbing structures. *Proc. Instn Mech. Engrs, Part C: J. Mechanical Engineering Science*, 1985, **199**, 121–131.
16 **Beevers, A.** and **Ellis, M. D.** Impact behaviour of bonded mild steel lap joints. *Int. J. Adhesion Adhes.*, 1984, **4**, 13–16.
17 **Kihara, K., Isono, H., Yamabe, H.,** and **Sugibayashi, T**. A study and evaluation of the shear strength of adhesive layers subjected to impact loads. *Int. J. Adhesion Adhes.*, 2003, **23**, 253–259.
18 **Adams, R. D.** and **Harris, J. A.** A critical assessment of the block impact test for measuring the impact strength of adhesive bonds. *Int. J. Adhesion Adhes.*, 1996, **16**, 61–71.
19 **Blackman, B. R. K., Kinloch, A. J., Taylor, A. C.,** and **Wang, Y.** The impact wedge peel performance of structural adhesives. *J. Mater. Sci.*, 2000, **35**, 1867–1884.
20 **Yokoyama, T.** Experimental determination of impact tensile properties of adhesive butt joints with the split Hopkinson bar. *J. Strain Analysis*, 2003, **38**, 233–245.
21 **Yokoyama, T.** and **Smitzu, H.** Evaluation of impact shear strength of adhesive joints with the split Hopkinson bar. *Jpn Soc. Mech. Engrs, A*, 1998, **41**, 503–509.
22 **Usui, Y.** and **Sakata, O.** Impact-fatigue strength of adhesive joints. *Jpn Soc. Proc. Engrs*, 1984, **18**(3), 213–218.
23 **Yu, J., Peter, K.,** and **Huang, M.** The impact-fatigue fracture of metallic materials. *JOM*, 1999, **51**, 15–18.
24 **Ninomi, M., Uwai, K., Kobayashi, T.,** and **Okahara, A.** Impact fatigue properties of epoxy resin filled with SiO_2 particles. *Eng. Fract. Mech.*, 1991, **38**, 439–449.
25 **Yamamoto, I., Higashihara, T.,** and **Kobayashi, T.** Effect of silica-particle characteristics on impact/usual fatigue properties and evaluation of mechanical characteristics of silica-particle epoxy resins. *Jpn Soc. Mech. Eng. A*, 2003, **46**, 145–153.
26 **Tanaka, T., Kinishita, K.,** and **Nakayame, H.** Effect of loading time on high-cycle range impact-fatigue strength and impact-fatigue crack growth rate. *Jpn Soc. Mech. Eng. I*, 1992, **35**, 108–116.
27 Test methods for fatigue properties of structural adhesives in tensile shear. 1995, ISO 9664:1995.
28 **Casas-Rodriguez, J. P., Ashcroft, I. A.,** and **Silberschmidt, V. V.** Damage evolution in adhesive joints subjected to impact fatigue. *J. Sound Vibr.*, 2007, **308**, 467–478.
29 **Takeshi, O.** *The fatigue behaviour of toughened epoxy polymers.* PhD Thesis, Imperial College of Science, London, 1999.
30 **Li, D., Yee, A. F., Chen, I.-W., Chang, S.-C.,** and **Takahashi, K.** Fracture behaviour of unmodified and rubber-modified epoxy under hydrostatic pressure. *J. Mater. Sci.*, 1994, **29**, 2205–2214.
31 **Casas-Rodriguez, J. P., Ashcroft, I. A.,** and **Silberschmidt, V. V.** Propagation of delamination zones in bonded joints. *Proc. Est. Acad. Sci., Phys. Math.*, 2007, **56**, 170–176.
32 **Sih, G. C.** and **Tang, X. S.** Random property of micro/macro fatigue crack growth behaviour predicted from energy density amplitude range. *Theor. Appl. Fract. Mech.*, 2007, **43**, 97–111.
33 **Moskala, E. J.** Effects of mean stress and frequency on fatigue crack propagation in rubber-toughened

polycarbonate/copolyester blends. *J. Appl. Polym. Sci.*, 1993, **49**, 53–64.

34 Jethwa, J. K. *The fatigue performance of adhesively-bonded metal joints*. PhD Thesis, Imperial College of Science, London, 1995.

35 Hwang, J. F., Manson, J. A., and **Hertzberg, R. W.** Fatigue crack propagation of rubber-toughened epoxies. *Polym. Eng. Sci.*, 1989, **29**, 1477–1487.

36 Slepyan, L. I. *Models and phenomena in fracture mechanics*, 2002 (Springer, Berlin and Heidelberg).